

Increasing shot and data collection rates of the Shock/Shear experiment at the National Ignition Facility

F. W. Doss, K. A. Flippo, D. Capelli, T. Cardenas, B. DeVolder, J. Kline, L. Kot, S. Kurien, E. Loomis, E. C. Merritt, T. Perry, D. Schmidt, and C. Di Stefano

Los Alamos National Laboratory, Los Alamos, NM 87545

E-mail: fdoss@lanl.gov

Abstract. Updates to the Los Alamos laser-driven high-energy-density Shock/Shear mixing-layer experiment are reported, which have collectively increased the platform's shot and data acquisition rates. The strategies employed have included a move from two-strip to four-strip imagers (allowing four times to be recorded per shot instead of two), the implementation of physics-informed rules of engagements allowing for the maximum flexibility in a shot's total energy and symmetry performance, and splitting the laser's main drive pulse from a monolithic single pulse equal to all beams into a triply-segmented pulse which minimizes optics damage.

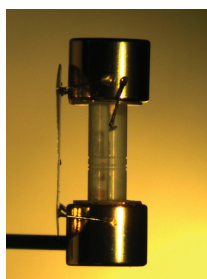


Figure 1. A LANL Shock/Shear target for NIF, with two indirect-drive halfraums on top and bottom and a BABL to the left. The visible portion of the shock tube is 5 mm tall.

1. Introduction

The Los Alamos National Laboratory (LANL) high-energy-density Shock/Shear experiment has used the National Ignition Facility (NIF) [1] at Lawrence Livermore National Laboratory (LLNL) to obtain shear-driven mixing data at high Atwood and Reynolds numbers. The Shock/Shear platform (Figure 1) is a shock tube filled by foam and separated by a dense material (typically aluminum) driven at each end by a halfraum, which launches shocks and drives hydrodynamic flow into the shock tube. When the shocks cross in the center of the tube, extremely strong shear is created, and the development of a temporally growing mixing layer is subsequently observed.



The Big Area BackLighter (BABL) radiography source [2], a foil mounted from the halfraums covering one side of the experiment, is then driven to provide x-ray illumination and diagnose the experiment. The platform development campaign covering the first five shots, along with many other details of the design and analysis methods discussed below, is fully documented in Doss et al [3].

Four major innovations have contributed to an increased rate of data acquisition:

- Moving from a two-strip radiography scheme to a four-strip, doubling the number of mixing-layer images which can be taken in a single shot.
- The implementation of physics-based constraints on drive energy and symmetry.
- Breaking up the main drive pulse into a three-part segmented drive to reduce the impact on laser optics of each shot.

Together with the facility's efforts to increase the overall NIF shot rate [4] by a factor of 1.5 from 2014 to 2015, the rate of usable data acquisition of the Shock/Shear experiment was increased by these improvements by a factor of ~ 6 . Below we will summarize the methods and impact of increasing the platform data output with these methods. In addition to increasing the quantity of radiography, the quality of data taken was also improved by a change from plastic to beryllium tubes for superior x-ray transmissibility. Improvements to target fabrication which allowed the move to beryllium tubes have been documented in Capelli et al. [5]. Statistics on the shots taken so far using the platform will also be given.

2. Four-strip radiography

During its initial platform development campaign, the Shock/Shear experiment could obtain two frames of data per experiment. The hGXD, a class of Gated X-ray Detector [6] which images onto film [7], can be outfitted with gated micro-channel plate stages which split the image into either two or four images taken at separate times.

For the platform development, shock timing and drive characterization required a full view of the target geometry. In addition to grids which can be used to determine magnification and, with preshot target metrology, absolute positioning of features with respect to the target ends, location-orienting notch fiducials were placed on the outer edge of the target volume and the shock's interaction with the wall was used to locate the shock. The radiography produced by the BABL used in this experiment was very spatially flat in intensity, which allowed this method to accurately locate the shocks.

The tradeoff in moving to the four-strip camera is that it reduces the imageable area to only that around the mixing layer. The drive conditions therefore had to be accurately characterized before this switch. Figure 2 shows an example of the reduced lateral span of the four-strip imaging scheme compared to the 2-strip shot N140923-2. The shock tube walls, and correspondingly the opportunity to register the shock location, are cut out. However, as can be seen in a subsequent image from shot N150415, the grid is positioned such that it is now imaged in an adjacent strip and can still be used in the four-strip configuration.

To fully take advantage of the additional data which can be taken in the four-strip configuration, the radiography scheme also needed to be extended to create a longer usable pulse of x-rays. This work is described in detail in Kirk Flippo's paper (this volume) [8].

3. Physics-based limits

As shots continued, it became necessary to define rules of engagement for each shot which allowed the maximum permissible variation in drive conditions while still maintaining physics fidelity. Compared to many other experiments on the NIF, the drive requirements in total energy are relatively loose for these shots, and have been quantified. Design calculations performed using the LANL hydrocode RAGE [9] and subsequently with the LLNL code KULL [10] identified a

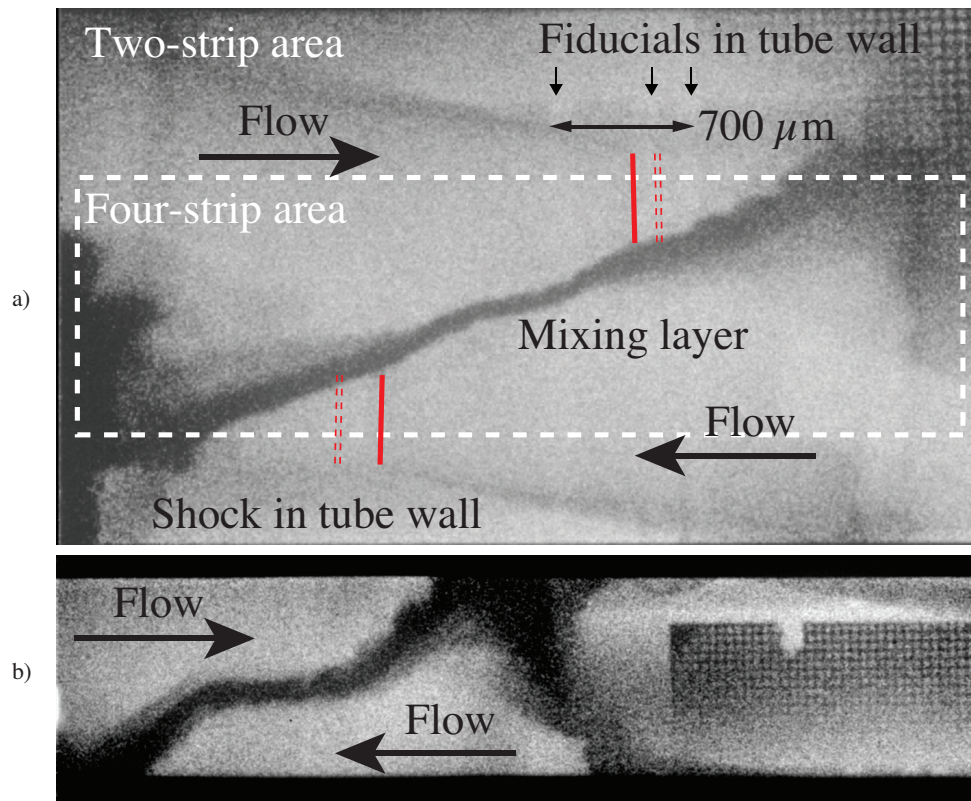


Figure 2. (a) Data from a single strip of Shot N140923-2 at 23 ns. Analysis of the radiography uses the machined fiducials and refracted components of shocks in the tube walls to determine the inferred shock locations (shown in red). The white rectangle shows the equivalent usable imaging area allowed by a single strip of the four-strip imager instead of the two-strip, discussed in Section 2. The dashed red lines show the shock locations measured in the cognate shot N141017 which fired with 611 kJ compared to this shot's 569 kJ (see Section 3 for discussion). Underneath, (b) shows a single strip from a four-strip shot (N150415 at 29.5 ns).

10% end-to-end drive asymmetry as sufficient to substantially modify the mixing dynamics at the center of the tube. This level of 10% is taken as the limiting factor past which the data has been corrupted and is likely unusable for precision mix measurements.

Figure 3 shows a collection of data from shots taken through January 2016. With the exception of several shots in which entire beams, quads (clusters of four beams), or bundles (pairs of quads linked between the top and bottom of the chamber) were lost, the data cluster near the design energy of 602 kJ (607 ± 7 kJ). Even in the cases of the experiments in which significant beam energy was lost (including the six named shots to the left of the main drive cluster), drive symmetry can be preserved. It is typically known leading up to the experiment if entire quads will be unable to fire; our rules of engagement, informed by the simulated limits at which the experiment can function, allow us to then drop a corresponding amount of energy from the opposite side. This has allowed us to keep drive symmetry between the top and the bottom halfraums to within 5% over all shots (providing a factor-of-two safety margin to the 10% limit at which it affects the mixing layer) at the cost of additional energy loss (but also keeping all shots within, to date, 8% of the nominal drive energy). The efficient use of these limits has allowed us to field experiments rapidly.

The second-to-left-most shot in Figure 3, shot N140923-2, was the last of the named “low-

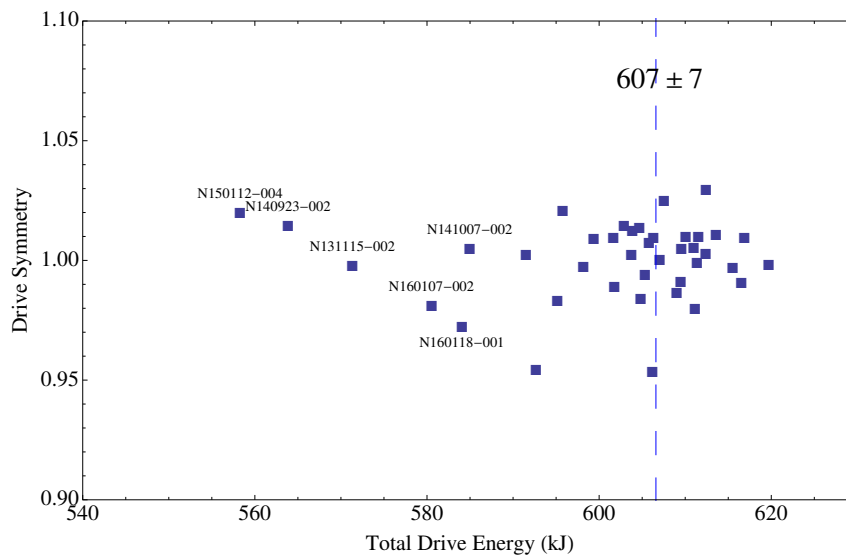


Figure 3. Drive energies in kilojoules for all fully-driven Shock/Shear NIF experiments through January 2016. The vertical axis shows drive symmetry between the top and bottom halfraums. The main cluster of shots is centered around 607 kJ with a spread of ± 7 kJ. Six shots in which the drive varied strongly due to entire dropped beams have been named explicitly to the left.

drive” shots to be imaged with the two-strip instead of the four-strip diagnostic discussed in Section 2 and the first shot designed to field the triply-segmented pulse described in Section 4. It is therefore an interesting shot for comparing the impact both of total energy and of the other changes discussed here. A full-power cognate shot, in which only the drive was varied, is N141017, which fired with 611 kJ. The shocks in N141017 were located (measured from the bottom surface of the shock tube) at $3073 \pm 13 \mu\text{m}$ and 1860 ± 60 for the top shock (which travels from 0 to 5 mm) and bottom shock (which travels in the opposite direction), respectively. In N140923-2, driven with 569 kJ, for data taken at the same time, we instead find positions of $2952 \pm 44 \mu\text{m}$ and $2067 \pm 21 \mu\text{m}$, respectively. This indicates a delay in shock position of 100-200 μm , or 2-4% of the length of the tube. This shock displacement is illustrated in Figure 2. For drive variations at this level, the final data analysis to be compared with simulation output should be expected to require comparable scaling of the shock and flow velocities. However, this was an extreme case, with a 7% discrepancy in delivered power; the vast majority of shots, which fell within 2% of the design energy, should exhibit no noticeable effects from their small changes in laser energy.

4. Pulse splitting

A major component in the scheduling and fielding of a NIF campaign is the burden of the shots to the NIF optics recycling program [11, 12]. The accumulation of optics damage is sensitive to the structure of the laser pulse [13], and the laser-optics modeling code LPOM [14] predicted that we could lower the costs of the laser drive with no impact (ideally) to its performance by using the modified drive pulse shown in Figure 4. This allowed the shot rate of the Shock/Shear experiment to nearly triple, by fielding more shots per given allocation of optics usage.

In Figure 4, the original single-shaped laser pulse which used 60 beams to drive each halfraum (available in [3]) has been split into three shorter component pulses, using 32, 16, and then 12 beams which sum to recreate the original platform drive pulse (shown in black). In order to maintain the same total power entering the halfraum, the power of each component beam was

increased, but this is more than compensated by the shortening of pulse duration during which the damage accumulates.

The tradeoff here is that optics damage has been exchanged for robustness against drive fluctuations. Previously, in the 60-beam pulse in which each beam participated equally, the loss of a four-beam quad would lead to an even 6% loss of power on that side over the entire pulse. With the split pulse, the loss of the same four beams can be as much as 30% of the power of the drive group. Worse, if the beams are lost from the second or third group, what was originally a flat or slowly decreasing beam profile becomes a modulated one possibly containing local increases, which can affect the mixing layer data if the imaging time of the experiment is sufficiently late. Without modifying the rules of engagement, based on the energy delivery statistics reported in Figure 3 we could expect loss of data due to loss of drive energy of 5-10%. Consequently, the triply-segmented pulse, while allowing for an increased shot rate, requires additional specification to the total energy and symmetry rules above; typically a quad loss is only permitted on the first, earliest group. For images sufficiently early in time (before 30 ns) it was determined by simulation that a single quad may be lost from the last pulse and the loss of energy will not propagate to the layer before the experiment ends.

The as-shot laser profiles for two shots are shown in Figure 4, averaging the top and bottom hohlraums together. The lower of the two curves is the record of shot N140923-2, the drive characterization shot for the triply-segmented pulse, which we have seen in Figure 2 and studied above as the lowest total energy shot (569 kJ) which was fired with the two-strip GXD. As can be seen, a significant drop occurred in the first pulse on each side, leading to a 7% overall loss to the total integrated energy, reflected in the delayed shock locations discussed above. We found however that the drive was consistently described just by the effects of this lowered energy, with no indication of transients or anomalous hydrodynamics caused by handing off one group of beams to the next.

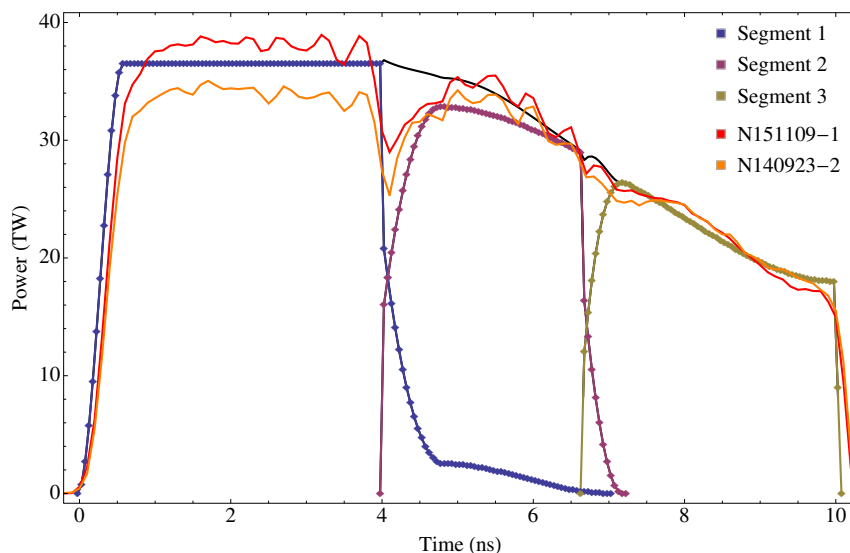


Figure 4. The three-stepped pulse used by the Shock/Shear experiments in 2015. The blue, purple, and tan dots show the drive pulse segments with 32, 16, and 12 beams respectively contributing to each segment on each side of the target. The black line shows the sum of the segments. The red curve shows the as-shot laser drive for a shot which performed well (N151109-1) and the orange curve shows a shot which underperformed (N140923-2). The total integrated design power of this pulse is 301 kJ from each side.

5. Summary

Following the platform development and scaling study reported in Doss et al [3], modifications to the Shock/Shear platform were made to increase the campaign's shot and data throughput. These included moving from two-strip to four-strip radiography (at the penalty of losing additional drive calibration information with each shot), implementing specific physics-informed rules of engagement (obtaining data which may require simulation-informed scaling in total energy to be properly folded into the complete shot sequence), and fielding a triply-segmented drive pulse to mitigate the campaign's optics damage budget (at the cost of increased risk to beam losses from the later segments). Through these improvements, the campaign has increased its data-taking rate by a factor of ~ 6 (three times as many shots for a given assignment of laser time, acquiring twice as much data per shot, reduced slightly by the need for tighter rules of engagement), which will be important to complete the high-Atwood and roughness scaling studies in progress in a timely fashion.

Acknowledgments

This work was supported by the U.S. Department of Energy and executed by Los Alamos National Laboratory under Contract DE-AC52-06NA25396. Experiments performed on the National Ignition Facility additionally reflect facility development and operations performed under the U.S. Department of Energy by Lawrence Livermore National Laboratory under Contract DE-AC52-07NA27344. This manuscript is numbered LAUR-16-20676.

References

- [1] Moses E I and Wuest C R 2003 *Fusion Science and Technology* **43** 420–427
- [2] Flippo K A, Kline J L, Doss F W, Loomis E N, Emerich M, Devolder B, Murphy T J, Fournier K B, Kalantar D H, Merritt E, Perry T S, Tregillis I, Welser-Sherrill L and Fincke J R 2014 *Review of Scientific Instruments* **85** 093501
- [3] Doss F W, Kline J L, Flippo K A, Perry T S, DeVolder B G, Tregillis I, Loomis E N, Merritt E C, Murphy T J, Welser-Sherrill L and Fincke J R 2015 *Physics of Plasmas* **22** 056303
- [4] Brunton G, Bowers G, Conder A, Nicola J D, Nicola P D, Fedorov M, Fishler B, Fleming R, Lau G, Kalantar D, Mathisen D, Miller-Kamm V, Pacheu V, Paul M, Reed R, Rouse J, Sanchez R, Shaw M, Stout E, Tang Y, Weaver S and Wilson R 2016 *Proceedings of ICALEPCS 2015, Melbourne, Australia* (Joint Accelerator Conferences Website) p MOD3O03
- [5] Capelli D, Schmidt D W, Cardenas T, Rivera G, Randolph R B, Fierro F, Merritt E C, Flippo K A, Doss F W and Kline J L 2016 *Fusion Sciences and Technology* **in press**
- [6] Oertel J A, Aragonz R, Archuleta T, Barnes C, Casper L, Fatherley V, Heinrichs T, King R, Landers D, Lopez F, Sanchez P, Sandoval G, Schrank L, Walsh P, Bell P, Brown M, Costa R, Holder J, Montelongo S and Pederson N 2006 *Review of Scientific Instruments* **77** 10E308
- [7] Glenn S, Bell P M, Benedetti L R, Bradley D K, Celeste J, Heeter R, Hagmann C, Holder J, Izumi N, Kilkenny J D, Kimbrough J, Kyrala G A, Simanovskaia N and Tommasini R 2011 *Penetrating Radiation Systems and Applications (Proceedings of SPIE vol 8144)* ed Grim G P and Schirato R C p 814409
- [8] Flippo K, DeVolder B, Doss F, Kline J, Merritt E, Loomis E, Capelli D, Schmidt D and Schmitt M J 2014 *J. Phys.: Conf. Ser.* **IFSA 2015** to be published
- [9] Gittings M, Weaver R, Clover M, Betlach T, Byrne N, Coker R, Dendy E, Hueckstaedt R, New K, Oakes W R, Ranta D and Stefan R 2008 *Computational Science and Discovery* **1** 015005
- [10] Rathkopf J A, Miller D S, Owen J M, Stuart L M, Zika M R, Eltgroth P G, Madsen N K, McCandless K P, Nowak P F, Nemanic M K, Gentile N A, and Keen N D 2000 KULL: LLNL's ASCI inertial confinement fusion simulation code Tech. Rep. UCRL-JL-137053 Lawrence Livermore National Laboratory
- [11] NIF and Photon Science 2016 National Ignition Facility User Guide Tech. Rep. LLNL-TM-681123-P2103437-WO15466-NUG Lawrence Livermore National Laboratory
- [12] Spaeth M L, Wegner P J, Suratwala T I, Nostrand M C, Bude J D, Conder A D, Folta J A, Heebner J E, Kegelmeyer L M, MacGowan B J, Mason D C, Matthews M J and Whitman P K 2016 *Fusion Science and Technology* **29** FST15–119
- [13] Carr C W, Trenholme J B and Spaeth M L 2007 *Applied Physics Letters* **90** 041110
- [14] Shaw M, House R, Williams W, Haynam C, White R, Orth C and Sacks R 2008 *Journal of Physics: Conference Series* **112** 032022